Report

Neuron

Stoichiometry and Phosphoisotypes of Hippocampal AMPA-Type Glutamate Receptor Phosphorylation

Highlights

- We estimated the stoichiometry and phosphoisotype of GluA1 phosphorylation
- Phosphorylation at S831 and S845 was almost negligible in adult hippocampus
- Dually phosphorylated GluA1 at both S831 and S845 could not be detected
- Our results impel us to reconsider the mechanisms underlying synaptic plasticity

Authors

Tomohisa Hosokawa, Dai Mitsushima, Rina Kaneko, Yasunori Hayashi

Correspondence

yhayashi@brain.riken.jp

In Brief

Hosokawa et al. estimated the proportion of phosphorylated AMPAR subunit GluA1 using Phos-tag SDS-PAGE. The level of phosphorylated GluA1 at S831 and S845, two major sites believed to be implicated in synaptic plasticity, was almost negligible.

Hosokawa et al., 2015, Neuron *85*, 60–67
January 7, 2015
http://dx.doi.org/10.1016/j.neuron.2014.11.026

CellPress

CellPress

Neuron
Report

Stoichiometry and Phosphoisotypes of Hippocampal AMPA-Type Glutamate Receptor Phosphorylation

Tomohisa Hosokawa,[1] Dai Mitsushima,[2,3] Rina Kaneko,[1] and Yasunori Hayashi[1,4,*]
[1]Brain Science Institute, RIKEN, Wako, Saitama 351-0198, Japan
[2]Department of Physiology, Yokohama City University Graduate School of Medicine, Yokohama, Kanagawa 236-0004, Japan
[3]Department of Systems Neuroscience, Yamaguchi University Graduate School of Medicine, Ube, Yamaguchi 755-8505, Japan
[4]Saitama University Brain Science Institute, Saitama University, Saitama 338-8570, Japan
*Correspondence: yhayashi@brain.riken.jp
http://dx.doi.org/10.1016/j.neuron.2014.11.026

SUMMARY

It has been proposed that the AMPAR phosphorylation regulates trafficking and channel activity, thereby playing an important role in synaptic plasticity. However, the actual stoichiometry of phosphorylation, information critical to understand the role of phosphorylation, is not known because of the lack of appropriate techniques for measurement. Here, using Phos-tag SDS-PAGE, we estimated the proportion of phosphorylated AMPAR subunit GluA1. The level of phosphorylated GluA1 at S831 and S845, two major sites implicated in AMPAR regulation, is almost negligible. Less than 1% of GluA1 is phosphorylated at S831 and less than 0.1% at S845. Considering the number of AMPAR at each synapse, the majority of synapses do not contain any phosphorylated AMPAR. Also, we did not see evidence of GluA1 dually phosphorylated at S831 and S845. Neuronal stimulation and learning increased phosphorylation, but the proportion was still low. Our results impel us to reconsider the mechanisms underlying synaptic plasticity.

INTRODUCTION

The phosphorylation of AMPAR has been proposed to play a critical role in synaptic plasticity (Derkach et al., 2007; Shepherd and Huganir 2007). The hypothesis involves the phosphorylation of AMPAR subunit GluA1 in a two-step process. Phosphorylation of S845 by PKA is a prerequisite for triggering AMPAR trafficking to the synaptic surface and maintenance during basal transmission (Lee et al., 2000; Esteban et al., 2003; Oh et al., 2006). Potentiation of synaptic transmission takes place when the receptor is additionally phosphorylated at S831 by CaMKII. This phosphorylation increases the single-channel conductance and contributes to the increased transmission following LTP induction (Benke et al., 1998; Derkach et al., 1999; Banke et al., 2000). In contrast, LTD is mediated by receptor removal caused by the dephosphorylation of S845-phosphorylated GluA1 at the synaptic surface (Kameyama et al., 1998; Lee et al., 2000). Overall, this scheme assumes that a large proportion of the GluA1 mediating synaptic transmission is phosphorylated. If LTP is maintained by phosphorylation of GluA1 at S831 and S845, one should be able to find dually phosphorylated GluA1 at these sites after LTP induction. Likewise, if dephosphorylation triggers removal of surface AMPAR during LTD, the majority of GluA1 maintaining basal transmission should be phosphorylated at S845. Phosphorylation at S818 controls the interaction with band 4.1N, a cytoskeletal anchoring protein, and those at T840 and S567 are also implicated in synaptic plasticity (Boehm et al., 2006; Delgado et al., 2007; Lee et al., 2007; Lu et al., 2010). Hence, multiple phosphorylation on GluA1 has been suggested to cooperatively participate in the induction and maintenance of synaptic plasticity.

However, critical information to attest this scheme, the stoichiometry of GluA1 phosphorylation and the phosphoisotypes (combination of phosphorylated sites) involved, are unknown. Several methods, including phosphospecific antibodies, phosphopeptide mapping, and mass spectrometry, have been used to detect the phosphorylation of specific sites. However, using these approaches, it is difficult to determine the proportion of phosphorylation and the phosphoisotypes. For example, western blotting with a phosphospecific antibody can detect a doubling of phosphorylation. However, it cannot distinguish whether the change is from 0.1% to 0.2% or from 10% to 20%. Also, it is very difficult to determine the phosphoisotype using phosphospecific antibodies. Because of this, although dually phosphorylated GluA1 at S831 and S845 is implicated in LTP, the presence of such receptor molecules has not been demonstrated. Therefore, critical experimental evidence to verify the aforementioned scheme is still lacking.

Phos-tag is a compound that associates with phosphate groups on a protein in the presence of divalent cations (Kinoshita et al., 2008; Hosokawa et al., 2010). When covalently conjugated with polyacrylamide in an SDS-PAGE, it separates phosphorylated from unphosphorylated proteins. Because the extent of separation is dependent on both the number of phosphorylated residues and the surrounding sequence, one can separate distinct phosphoisotypes of a given protein based on mobility. Furthermore, by blotting the gel with an appropriate antibody, one can also determine the stoichiometry of different phosphoisotypes.

Using this feature of Phos-tag SDS-PAGE, we quantified GluA1 phosphorylation in both mature and developing hippocampus.

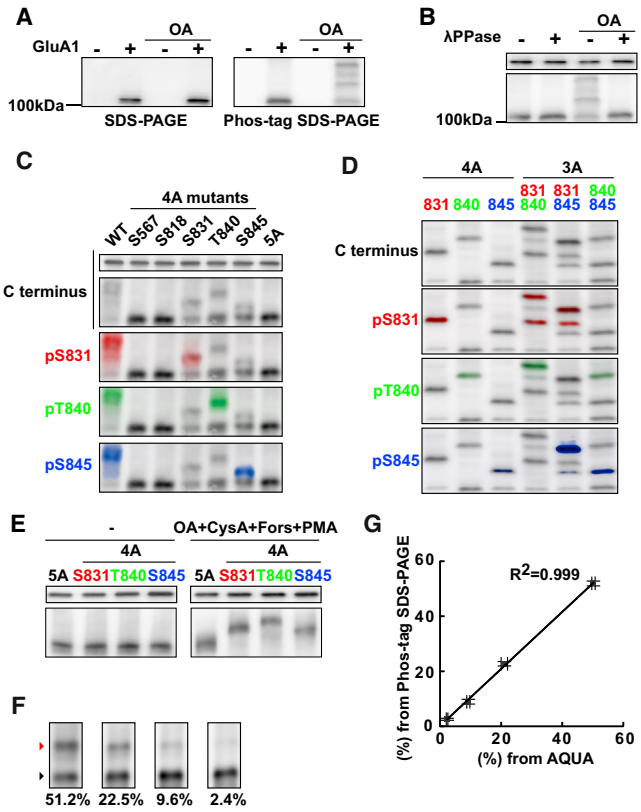

Figure 1. Separation and Quantification of Phosphoisotypes of GluA1 Using Phos-tag SDS-PAGE

(A) HEK293T cells expressing GluA1 were incubated with or without 1 μM okadaic acid (OA) for 4 hr. The homogenate was separated using conventional (left) or Phos-tag (right) SDS-PAGE and blotted with an antibody against the C terminus of GluA1. (B) Pretreatment of the sample with λ protein phosphatase (λPPase) abolishes the band shift. (C) Wild-type (WT) GluA1, four alanine mutants (4A) containing mutations in all but one out of five known sites, or a mutant where all known phosphorylation sites were mutated to alanine (5A) were expressed in HEK293T cells. To maximally induce phosphorylation, a constitutively active CaMKII was cotransfected, and the cells were further treated with forskolin, phorbol 12-myristate 13-acetate, cyclosporine A, and OA for 2 hr. The cell homogenate was separated using Phos-tag SDS-PAGE and blotted with antibodies against GluA1 C terminus, pS831, pT840, and pS845. (D) Detection of dually phosphorylated GluA1. 4A and three alanine (3A) mutants were expressed in HEK293T cells and phosphorylated as in (C). The numbers above the blot indicate phosphorylatable sites. (E) Sensitivity of C terminus antibody to phosphorylated GluA1. HEK293T cells expressing indicated mutants were treated as in (C), but for a longer duration (6 hr) to ensure complete phosphorylation. Then either unphosphorylated (left) or phosphorylated (right) AMPARs were separated using conventional SDS-PAGE (top) or Phos-tag SDS-PAGE (bottom) and blotted with the C terminus antibody. (F) GluA1 samples containing different amounts of pS831 GluA1 (on a 4A background) made by mixing different amounts of immunoprecipitated GluA1 from transfected HEK293T cells untreated or treated with OA. The mixtures were separated on Phos-tag SDS-PAGE and blotted with the C terminus antibody. The proportion of pS831 GluA1 in each sample is shown. The same samples were subjected to AQUA (Figures S1B–S1D). (G) Correlation of the result of Phos-tag SDS-PAGE (F) and AQUA (Figure S1D) in the stoichiometry of pS831 GluA1. n = 3, each.

We found that the stoichiometry of phosphorylation in adult tissue is much lower than expected from the current plasticity model. We did not find any evidence of GluA1 dually phosphorylated at both S831 and S845. Our results compel us to reevaluate the current model of AMPAR regulation.

RESULTS

Phos-tag SDS-PAGE Separates GluA1 Phosphorylated at Different Sites

To test whether Phos-tag SDS-PAGE is applicable for the analysis of GluA1 phosphoisotypes, GluA1 was expressed in HEK293T cells, and phosphorylation was induced by blocking endogenous phosphatase activity with okadaic acid (OA), an inhibitor of protein PP1 and 2A. This treatment increased the phosphorylation of various proteins in HEK293T cells (Figure S1A available online), likely by unmasking the basal activity of endogenous kinases. While GluA1 on conventional SDS-PAGE did not show a difference in migration in the presence or absence of OA, it showed multiple bands that migrated slowly only in the presence of OA on Phos-tag SDS-PAGE (Figure 1A). These bands disappeared by treating the cell lysate with λ protein phosphatase (Figure 1B).

To test whether the band shift was caused by phosphorylation at a previously identified GluA1 site, we mutated all five known phosphorylation sites to alanine (Figure 1C, 5A). The GluA1 wild-type or 5A mutant was coexpressed with a constitutively active form of CaMKII (phosphorylates GluA1 at S567 and S831), and the cells were further treated with phorbol ester (PKC activator, S818, S831, and T840), forskolin (PKA activator, S845), cyclosporine A (PP2B inhibitor), and OA (Barria et al., 1997; Lu et al., 2010; Roche et al., 1996; Boehm et al., 2006). Unlike wild-type GluA1, 5A mutants did not show a band shift indicating that there were no other phosphorylation sites under this condition.

To identify the phosphorylation sites causing the band shift, we mutated each of the alanine residues back to serine or threonine, while maintaining the other four alanines (4A mutants). S831, T840, and S845 on a 4A background showed a clear band shift, but at different positions. They were confirmed to be GluA1 phosphorylated at respective sites by blotting with phosphoantibodies. In contrast, S567 or S818 on a 4A background did not show a noticeable band shift. Also, an antibody against pS567 (Lu et al., 2010) did not detect any phosphorylated proteins, indicating a low phosphorylation stoichiometry (data not shown). As a result, we did not investigate the S567 and S818 phosphorylation sites further and focused on S831, T840, and S845.

To test if GluA1 dually phosphorylated at S831 and S845 could be detected, we made a construct that maintained both S831 and S845, but mutated the other three sites to alanine (Figure 1D, 3A 831+845). Blotting with a C terminus antibody detected GluA1 phosphorylated at S831 and S845 as well as unphosphorylated protein. Additionally, we detected a band above S831, which was confirmed to be dually phosphorylated GluA1 in the blots with pS831 and pS845 antibodies. This band was at almost the same location as singly phosphorylated GluA1 at T840. Therefore, for the rest of the study, we routinely reblotted

the membrane with phosphospecific antibodies to identify the phosphoisotype of each band.

Likewise, both individually and dually phosphorylated GluA1 were detected in S831 and T840 on a 3A background (the T840 band could be visualized using the C terminus antibody, but was too faint in the pT840 blot; Figure 1D). In the T840 and S845 on a 3A background, individually phosphorylated bands, but not dually phosphorylated bands, were detected. In summary, Phos-tag SDS-PAGE in combination with phosphospecific antibodies allows us to detect the phosphoisotypes of singly and dually phosphorylated GluA1.

Estimation of Phosphorylation Stoichiometry Using Phos-tag SDS-PAGE

Next we tested if we could use Phos-tag SDS-PAGE to determine the stoichiometry of GluA1 phosphorylation. For this purpose, we first ascertained whether the GluA1 C terminus antibody detects each phosphoisotype with equal efficiency. We maximally phosphorylated GluA1 mutants 5A or S831, T840, and S845 on 4A background and tested the reactivity of the antibody (Figure 1E). Phos-tag SDS-PAGE confirmed that they were ~100% phosphorylated. In these samples, there were no obvious differences in band intensity between the 5A and phosphorylated mutants, confirming that phosphorylation at S831, T840, and S845 did not affect the reactivity of the C terminus antibody.

We therefore assumed that, by comparing the intensity of the bands corresponding to phosphorylated and unphosphorylated GluA1 in the blot with C terminus antibody, we could estimate the stoichiometry of GluA1 phosphorylation using Phos-tag SDS-PAGE. To test this, we compared the result of quantification using Phos-tag SDS-PAGE with that of mass spectrometric absolute quantification (AQUA) (Gerber et al., 2003). We immunoprecipitated GluA1 (S831 on 4A background) from HEK293T cells, untreated or treated with OA, and mixed them at different ratios, thereby making a series of GluA1 samples with different stoichiometry of S831 phosphorylation. The stoichiometry of S831-phosphorylated GluA1 in each mixture was determined by western blotting with the C terminus antibody and measuring the band intensity of S831-phosphorylated and unphosphorylated GluA1 on the Phos-tag SDS-PAGE (Figure 1F). In parallel, the same samples were subjected to AQUA using a synthetic standard of phosphorylated and unphosphorylated peptides containing ^{13}C and ^{15}N (Figure S1D). The results from these two methods coincide with each other precisely (Figure 1G), indicating that Phos-tag SDS-PAGE is a reliable measure of the stoichiometry of protein phosphorylation.

Quantitative Analysis of GluA1 Phosphorylation in Hippocampus

We next determined the amount of phosphorylated GluA1 in adult rat hippocampus. In conventional SDS-PAGE, blotting with antibodies against GluA1 C terminus, pS831, pT840, and pS845 showed bands at the expected molecular weight (Figure 2A, top). As expected, upon phosphatase treatment, the bands disappeared from the blots using phosphoantibodies. Using Phos-tag SDS-PAGE, we observed a discrete band shift with pS831, pT840, and pS845 antibodies at similar relative positions as HEK293T cells (Figure 2A, bottom). However, when blotting was performed with the C terminus antibody, < 1% of pS831 and ~5% of pT840 GluA1 were detected at the corresponding positions, and pS845 was undetectable (Figure 2A, bottom, B and C). The dually phosphorylated GluA1 at S831 and S845 is expected to be at almost the same location as T840-phosphorylated GluA1 (Figure 1D), but, as there was no signal on the pS831 and pS845 blots (Figure 2A), we concluded that the upper band in the blot with C-terminal antibody was composed solely of pT840 GluA1. Likewise, there was no evidence of other multiply phosphorylated GluA1.

We also subjected hippocampal GluA1 to AQUA. Consistent with the result of Phos-tag SDS-PAGE, it also showed that pS831 on GluA1 from hippocampal tissue was barely detectable, an amount that was significantly lower than the smallest standard (2.3%) (Figure S1D). Changes in sample preparation method did not change the level of phosphorylation (Figure S2A). Therefore it is unlikely that GluA1 is dephosphorylated during sample preparation.

To further extend the dynamic range, we calibrated the immunoblot signal as follows. The 4A mutant samples containing ~100% phosphorylated receptors (Figure 1E) were serially diluted, separated using conventional SDS-PAGE, and blotted with phosphoantibodies, from which a calibration line was drawn (Figures 2D and 2E). Hippocampal extract, preadjusted so that it contains the same amount of total GluA1 (Figure 2D, bottom), was also separated on the same gel, and the amount of phosphorylated GluA1 at each site was obtained from the calibration line (Figures 2D, top, and 2E). We estimated that 0.18% ± 0.01%, 4.3% ± 0.7%, and 0.018% ± 0.001% of hippocampal GluA1 was phosphorylated at S831, T840, and S845, respectively (Figures 2D and 2E), largely consistent with the measurement of band intensity on Phos-tag SDS-PAGE.

One reason why only a small proportion of phosphorylated GluA1 was detected may be because the extract is a mixture of various membranous compartments. We therefore extracted the PSD fraction by detergent treatment, which is enriched with PSD-95, a prominent PSD protein, but lacks synaptophysin, a presynaptic protein (Figure 2F). Phos-tag SDS-PAGE revealed that the phosphorylation of GluA1 was not significantly different from other fractions. We also attempted to isolate surface GluA1 from cultured hippocampal neurons using a surface biotinylation and avidin pull-down (Figure 2G). There was no obvious difference in phosphoisotypes between internal and surface GluA1.

We next tested the ontogeny of GluA1 phosphorylation. The GluA1 phosphorylation was highest at P1 (Figures 2H and 2I). This was evident for pS831, which was 36.2 ± 1.3-fold higher at P1 compared with adult tissue. The level gradually diminished during development and reached adult levels by P28. We found that ~7% and ~25% of GluA1 is phosphorylated at S831 and T840, respectively, at P1 (Figures S2B and S2C). In addition, ~2.5% of GluA1 was dually phosphorylated at both S831 and T840. However, the level of S845-phosphorylated GluA1 was still low, as indicated by the lack of a band detected by the N terminus antibody at the corresponding position in the pS845.

We also analyzed other postsynaptic proteins in the hippocampus (Figure S2D). We found that a significant proportion of

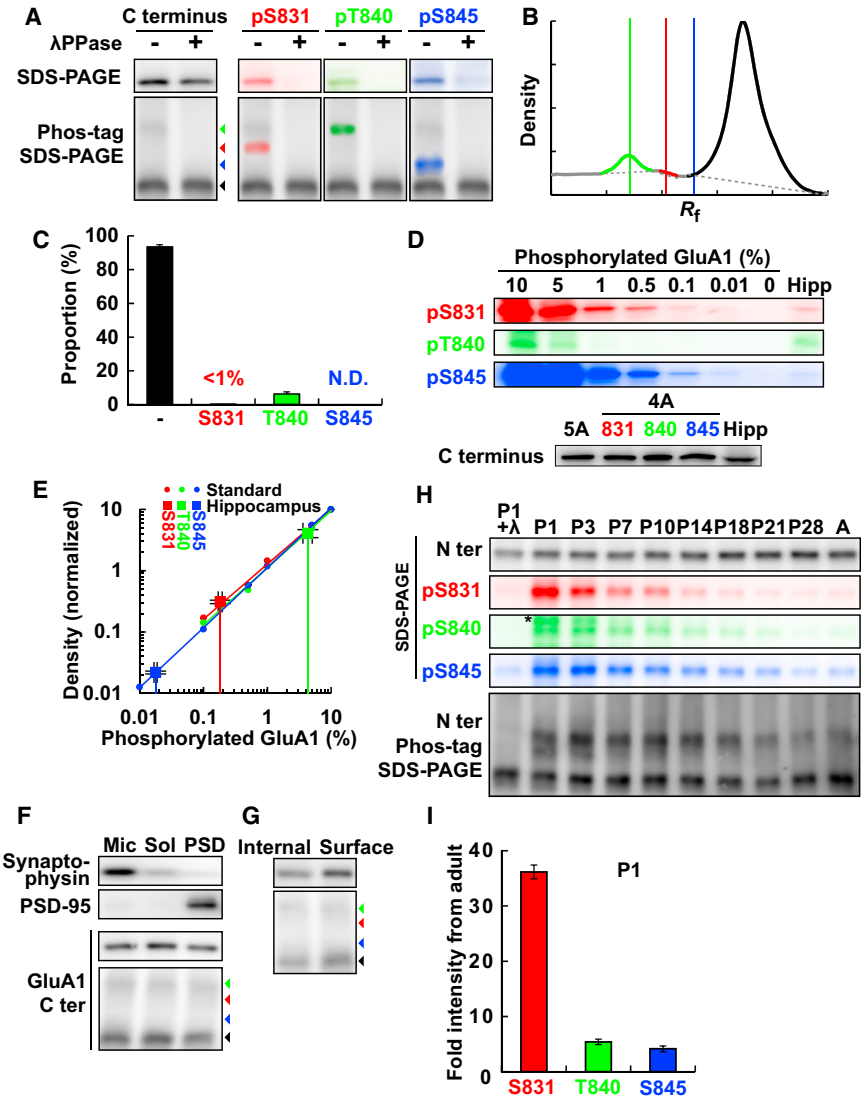

Figure 2. Endogenous GluA1 in Neurons Is Mostly Unphosphorylated

(A) Phosphoisotypes of endogenous GluA1 in adult rat hippocampus. Hippocampal extract was subjected to conventional SDS-PAGE (top) or Phos-tag SDS-PAGE (bottom) and blotted with antibodies against GluA1 C terminus, pS831, pT840, and pS845. (B) The densitometric profile of blots of hippocampal extract. The positions of pS831, pT840, and pS845 phosphoisotypes are shown by red, green, and blue lines, respectively. (C) Quantification of the population of each phosphoisotype. The pS831 was below the level where it could be confidently quantified (< 1%), and pS845 was not detected. (D) Blots of the dilution series of maximally phosphorylated 4A mutants on a conventional SDS-PAGE. Endogenous GluA1 from adult rat hippocampus was loaded on the right lane. Only one rat out of six is shown. A blot with the C terminus antibody (bottom) was used to adjust the total amount of GluA1. (E) Calibration of band density and amount of phosphorylated protein. The densitogram reading was normalized by the 10% phosphorylated sample. Squares are averages of six samples. (F) GluA1 phosphorylation in different subcellular fractions. The fractions from adult rat hippocampi were subjected to SDS-PAGE or Phos-tag SDS-PAGE and blotted with an anti-GluA1 C terminus. The amount of total GluA1 is preadjusted by performing a separate blot (data not shown). (G) Comparison of intracellular and neuronal surface GluA1 phosphoisotypes. The surface fraction was obtained from dissociated neuronal cultures by surface biotinylation and avidin pull-down. The remaining fraction was used as the intracellular fraction. (H) Ontogeny of GluA1 phosphorylation from P1 to adult hippocampus. Hippocampal homogenate from animals at various ages was separated by conventional and Phos-tag SDS-PAGE and blotted with indicated antibodies. We used the N terminus antibody because the C terminus antibody produced a nonspecific band in the P1 sample (data not shown). Also, the uppermost band with * in the pT840 blot represents cross-reactivity, as it was not detected with the N terminus antibody. See Figure S2C for identification of phosphoisotypes. The amount of total GluA1 is preadjusted by performing a separate blot (data not shown). (I) Quantification of phosphorylation in P1 hippocampus. The level is expressed as adult levels as one. The original image is in Figure S2B. The level of pT840 may be an overestimation due to cross-reactivity shown with * in the pT840 blot in Figure S2B. n = 5.

GluN2B was phosphorylated at tyrosine sites in both P1 and adult hippocampal tissue, though we did not attempt to determine the exact site. Almost all stargazin in adult PSD fraction was phosphorylated, consistent with an earlier study (Sumioka et al., 2010). A minor population of PSD-95 was phosphorylated in adult tissue, possibly at S73 or S295 (Kim et al., 2007; Steiner et al., 2008). Likewise, a minor population of cofilin was phosphorylated at S3 both in P1 and adult tissue. These data demonstrate the versatility of Phos-tag SDS-PAGE in estimating the stoichiometry of phosphorylation of various proteins.

GluA1 Phosphorylation in Chemical LTP

We next attempted to test if the level of GluA1 phosphorylation changes by stimulating neurons. We induced chemical LTP (chemLTP) in dissociated neuronal cultures by applying a saturating concentration of glycine (Lu et al., 2001). Following the stimulation, the levels of surface GluA1 were increased by 1.43 ± 0.12-fold (Figures 3A and 3B) as reported (Lu et al., 2001). Concomitantly, pS831 and pS845 GluA1 on the cell surface increased significantly beyond the increase in total surface GluA1, indicating a net increase in the proportion of phosphorylated GluA1 (Figures 3A–3C). However, the proportion of phosphorylated cell surface GluA1 still remained low, from 0.16% ± 0.02% before stimulation to 0.25% ± 0.02% after chemLTP induction at S831, and from 0.012% ± 0.001% to 0.047% ± 0.002% at S845 (Figures 3D–3F).

The low amount of phosphorylated GluA1 may be due to rapid dephosphorylation. We therefore treated the cells with phosphatase inhibitors. Treatment of unstimulated neurons led to a significant increase in phosphorylated receptors

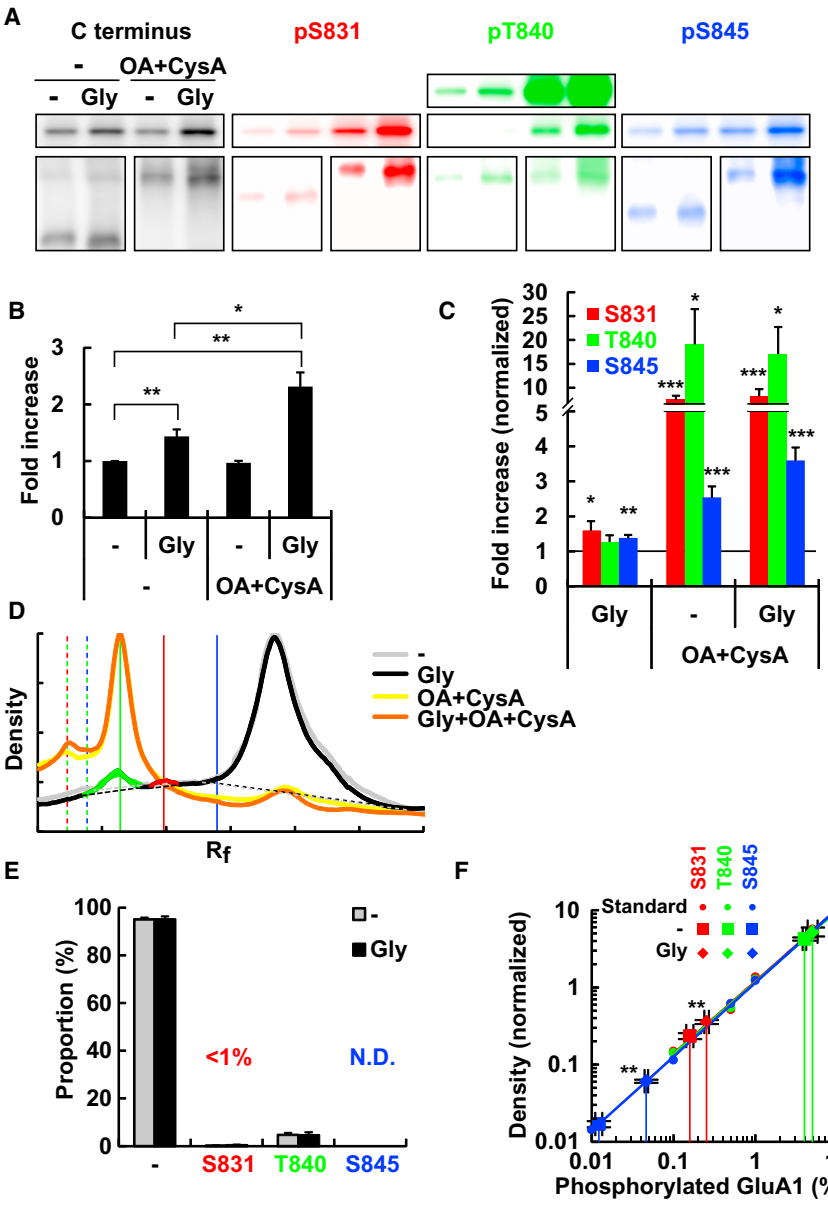

Figure 3. Glycine-Induced Chemical LTP Increases Phosphorylation of Cell Surface GluA1, but the Absolute Proportion of the Phosphorylated Population Is Low

(A) Dissociated neuronal cultures were treated with glycine to induce chemLTP in the absence (–) or presence of okadaic acid and cyclosporine A (OA+CysA). Surface GluA1 was obtained by surface biotinylation and avidin pull-down. The samples were subjected to SDS-PAGE (top) or Phos-tag SDS-PAGE (bottom) and blotted with indicated antibodies. Each Phos-tag SDS-PAGE blot had a different exposure time and therefore cannot be cross-compared. (B) Quantification of the surface GluA1 confirms successful induction of chemLTP. (C) Amount of phosphorylation normalized by the amount of surface GluA1. The level was determined from the density of conventional SDS-PAGE in (A). (D) The densitometoric profile of Phos-tag SDS-PAGE. (E) Quantification of data in (C). The peaks at S831 and S845 are below the amount that can be confidently quantified. (F) The amount of phosphorylated GluA1 before and after chemLTP induction plotted on calibration line of the dilution series. *$p < 0.05$, **$p < 0.01$, ***$p < 0.001$ (two-tailed t test). n = 6 for (B)–(F).

(Figures 3A, 3C, 3D, and S3A). This was mostly due to pT840, which increased by 19.1 ± 7.3-fold of basal levels and reached ~80% of the total GluA1, indicating that T840 is undergoing a constant phosphorylation-dephosphorylation cycle during basal states (Figures 3A, 3C, 3D, and S3). pS831 increased by 7.54 ± 0.81-fold and pS845 by 2.54 ± 0.31-fold (Figures 3A, 3C, and S3B), but they still only account for a small proportion (Figure S3C). Also, treatment with the phosphatase inhibitor itself did not increase surface GluA1 levels (Figures 3A and 3B).

When phosphatase inhibitors were combined with glycine, it increased the surface GluA1 by 2.31 ± 0.25-fold, while the increase was only 1.43 ± 0.12-fold with glycine alone (Figures 3A and 3B). However, the effect on phosphorylation of cell surface GluA1 was still small. pS831 and pT840 did not increase further, and S845 marginally increased (Figures 3C and 3D). In summary, T840 undergoes cycles of phosphorylation-dephosphorylation under basal conditions, with endogenous phosphatase activity maintaining phosphorylation at low levels. In contrast, the kinase activity to phosphorylate S831 and S845 is intrinsically low, at both basal states and during chemLTP induction, and it is not phosphatase activity that maintains low levels of phosphorylation.

GluA1 Phosphorylation in Inhibitory Avoidance Learning

To examine GluA1 phosphorylation in vivo, PSD fractions of hippocampal tissue from rats that underwent inhibitory avoidance learning were analyzed. This paradigm induces a rapid and persistent potentiation of hippocampal synaptic transmission both in vitro and in vivo (Whitlock et al., 2006; Mitsushima et al., 2011, 2013). We found a 2.5-fold increase in AMPA/NMDA ratio, a 33% increase in miniature EPSC amplitude, and a 54% increase in frequency in randomly sampled cells compared with tissue from control animals, indicating that a significant proportion of synapses undergo potentiation with this paradigm. We prepared PSD fractions from rats before, 5 min after, and 30 min after training, when an increase in transmission was observed. The training induced an increase in pS831 and pS845 GluA1 in the PSD fraction, consistent with earlier studies (Whitlock et al., 2006; Mitsushima et al., 2011), but not in pT840 (Figures 4A and 4B). However, when compared with the total levels of GluA1 in the PSD fraction, the amount of phosphorylated GluA1 at these sites was still

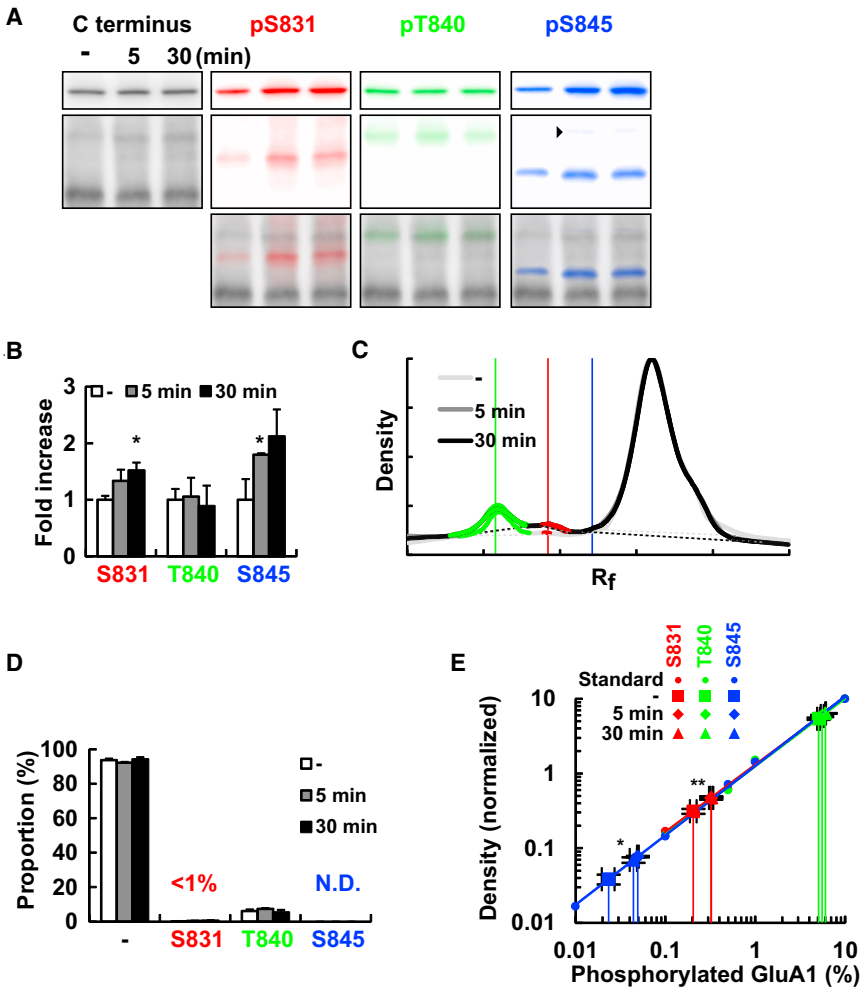

Figure 4. Inhibitory Avoidance Conditioning Increases GluA1 Phosphorylation, but the Absolute Proportion of Phosphorylated Population Is Low

Rats were subjected to the inhibitory avoidance paradigm. At 5 or 30 min after conditioning, dorsal hippocampi were dissected, and the fraction insoluble to 1% Triton X-100 was isolated. (A) Blotting in SDS-PAGE (top) and Phos-tag SDS-PAGE (bottom). One rat from each group is shown. The top bands (arrowhead) of the pS845 blot (A) most likely represent a dually phosphorylated population at T840 and S845, but because the amount was small (< 0.01%), they were not analyzed. (B) Quantification of phosphorylation using a phosphospecific antibody normalized to the level observed in naive animals. Blotting in conventional SDS-PAGE was used for the quantification. (C) The densitometric profile of Phos-tag SDS-PAGE. (D) Quantification of data in (C). (E) The amount of phosphorylated GluA1 before and after inhibitory avoidance learning is plotted on calibration line of the dilution series. *$p < 0.05$, **$p < 0.01$ (two-tailed t test). A total of nine rats were separated into three groups.

low (Figures 4C–4E). It was 0.21% ± 0.02% under basal conditions and 0.33% ± 0.01% 30 min after learning for S831 and 0.023% ± 0.004% and 0.044% ± 0.004% for S845.

DISCUSSION

The stoichiometry of phosphorylation and phosphoisotypes of GluA1, two critical pieces of information to attest the importance of AMPAR phosphorylation in synaptic plasticity, have been overlooked so far, in part due to the lack of an appropriate method to obtain such information. Using Phos-tag SDS-PAGE, we found that the amount of phosphorylated GluA1 was very low. In naive hippocampal tissue, 0.18% and 0.018% of GluA1 was phosphorylated at S831 and S845, respectively. If we assume that there are 100 GluA1 molecules on each synapse (Tanaka et al., 2005; Sheng and Hoogenraad 2007), on average, only 1 out of ~6 synapses contains single pS831 GluA1 and 1 out of ~60 for pS845. Hence, the majority of GluA1 at synapses are not phosphorylated, and the rest of the synapses do not contain any phosphorylated GluA1. We also saw no evidence of dually phosphorylated GluA1 at S831 and S845.

In light of these results, the current model of plasticity, which assumes AMPAR phosphorylation plays a significant role, needs to be reevaluated. First, it is difficult to explain how LTP maintenance is linked with an increase in phosphorylation. GluA1 phosphorylation at S831 increases channel conductance only by ~2-fold (Derkach et al., 1999). Such an effect would be diluted by unphosphorylated AMPARs, which make up the majority of the AMPAR population. One possibility is that transient phosphorylation might be sufficient to induce LTP. However, we ruled out this possibility by treatment with a phosphatase inhibitor, which only marginally increased S831 and S845 phosphorylation upon glycine treatment. Similarly, the majority of synapses do not contain even a single S845-phosphorylated GluA1. This observation rules out the possibility that LTD is mediated by dephosphorylation of synaptic GluA1.

Our estimation is in contrast with Oh et al. (2006) who found that ~15% of surface AMPARs were phosphorylated at S845 during basal conditions and increased to ~60% following chemLTP. They used a GST-fusion protein of GluA1 C terminus, phosphorylated to ~100%, as a standard. However, they introduced a P842R mutation to make it an efficient substrate of PKA. This manipulation may change the antigenicity of the fusion protein to the pS845 antibody and cause inaccuracy. Also, quantification of pS845 with the incorporation of ^{32}P may be compromised by possible phosphorylation at other sites, for example, T840. Finally, to induce chemLTP, they used forskolin/rolipram, which stimulates PKA, whereas we stimulated NMDA receptors with glycine.

T840 was the only site whereby a significant proportion of GluA1 was phosphorylated. However, glycine treatment only slightly increased pT840 GluA1 (1.27 ± 0.17-fold, statistically insignificant), and inhibitory avoidance training did not affect pT840 level. Even though we saw an ~20-fold increase in pT840 level after treatment with a phosphatase inhibitor, it still did not change the amount of cell surface GluA1. Also, T840A knock-in animals, with S838A, S839A, and additional S831A/S845A mutations, did not show any further phenotype compared with S831A/S845A knock-in (Lee et al., 2007). Therefore, the functional significance of this phosphorylation requires further study.

The impairment of synaptic plasticity in the S831A/S845A knock-in mutant GluA1 mice is generally accepted as strong evidence supporting the requirement of receptor phosphorylation (Lee et al., 2003). Studies using exogenous mutant receptors support this view (Esteban et al., 2003; Miyazaki et al., 2012; but see Hayashi et al., 2000). We indeed observed a significant increase in phosphorylation at S831 and S845 along with an increase in the surface GluA1 as a result of chemLTP or learning (Figures 3 and 4). Therefore, we need to find alternative interpretations for the role of GluA1 phosphorylation. First, phosphorylation in a small proportion of GluA1 may be sufficient to trigger changes in the population of unphosphorylated AMPAR. Alternatively, GluA1 phosphorylation may be important for normal synaptic development, when the GluA1 phosphorylation levels were high (Figure 2H) (Li et al., 2003). Impairment of the process may later manifest as an impairment in synaptic plasticity. Finally, these residues may be required for other protein interactions or forms of posttranslational modification. Recently, it was proposed that LTP does not require the carboxyl-tail of AMPA receptor. GluA1 lacking carboxyl-tail containing these phosphorylation sites or GluA2 with a carboxyl-tail of distinct amino acid sequence can replace wild type GluA1 (Granger et al., 2013). Together, these results compel us to consider what is the true mechanism of synaptic plasticity.

EXPERIMENTAL PROCEDURES

All gene recombinant and animal experiments were in accordance with the institutional guidelines of the RIKEN, Yokohama City University, and Yamaguchi University. All experimental procedures can be found in Supplemental Experimental Procedures.

SUPPLEMENTAL INFORMATION

Supplemental Information includes three figures and Supplemental Experimental Procedures and can be found with this article online at http://dx.doi.org/10.1016/j.neuron.2014.11.026.

ACKNOWLEDGMENTS

We thank Akane Shibuya and Yuki Okumura-Takayagi for assistance and Drs. Katherine Roche, Roger Nicoll, Takeo Saneyoshi, Kaori Otsuki, Masaya Usui, Eiji Kinoshita, Takuya Takahashi, Masaki Matsumoto, Takashi Hayashi, Steve Heinemann, John Lisman, and Lily Yu for sharing resources and comments on the manuscript. This work was supported by RIKEN, NIH grant R01DA17310, and Grant-in-Aid for Scientific Research (A) and Grant-in-Aid for Scientific Research on Innovative Area "Foundation of Synapse and Neurocircuit Pathology" from the MEXT, Japan (Y.H.). Y.H. is partly supported by a research grant from Takeda Pharmaceutical and Fujitsu Laboratories.

Accepted: November 13, 2014
Published: December 18, 2014

REFERENCES

Banke, T.G., Bowie, D., Lee, H., Huganir, R.L., Schousboe, A., and Traynelis, S.F. (2000). Control of GluR1 AMPA receptor function by cAMP-dependent protein kinase. J. Neurosci. *20*, 89–102.

Barria, A., Derkach, V., and Soderling, T. (1997). Identification of the Ca^{2+}/calmodulin-dependent protein kinase II regulatory phosphorylation site in the α-amino-3-hydroxyl-5-methyl-4-isoxazole-propionate-type glutamate receptor. J. Biol. Chem. *272*, 32727–32730.

Benke, T.A., Lüthi, A., Isaac, J.T., and Collingridge, G.L. (1998). Modulation of AMPA receptor unitary conductance by synaptic activity. Nature *393*, 793–797.

Boehm, J., Kang, M.G., Johnson, R.C., Esteban, J., Huganir, R.L., and Malinow, R. (2006). Synaptic incorporation of AMPA receptors during LTP is controlled by a PKC phosphorylation site on GluR1. Neuron *51*, 213–225.

Delgado, J.Y., Coba, M., Anderson, C.N., Thompson, K.R., Gray, E.E., Heusner, C.L., Martin, K.C., Grant, S.G., and O'Dell, T.J. (2007). NMDA receptor activation dephosphorylates AMPA receptor glutamate receptor 1 subunits at threonine 840. J. Neurosci. *27*, 13210–13221.

Derkach, V., Barria, A., and Soderling, T.R. (1999). Ca^{2+}/calmodulin-kinase II enhances channel conductance of α-amino-3-hydroxy-5-methyl-4-isoxazole-propionate type glutamate receptors. Proc. Natl. Acad. Sci. USA *96*, 3269–3274.

Derkach, V.A., Oh, M.C., Guire, E.S., and Soderling, T.R. (2007). Regulatory mechanisms of AMPA receptors in synaptic plasticity. Nat. Rev. Neurosci. *8*, 101–113.

Esteban, J.A., Shi, S.H., Wilson, C., Nuriya, M., Huganir, R.L., and Malinow, R. (2003). PKA phosphorylation of AMPA receptor subunits controls synaptic trafficking underlying plasticity. Nat. Neurosci. *6*, 136–143.

Gerber, S.A., Rush, J., Stemman, O., Kirschner, M.W., and Gygi, S.P. (2003). Absolute quantification of proteins and phosphoproteins from cell lysates by tandem MS. Proc. Natl. Acad. Sci. USA *100*, 6940–6945.

Granger, A.J., Shi, Y., Lu, W., Cerpas, M., and Nicoll, R.A. (2013). LTP requires a reserve pool of glutamate receptors independent of subunit type. Nature *493*, 495–500.

Hayashi, Y., Shi, S.H., Esteban, J.A., Piccini, A., Poncer, J.C., and Malinow, R. (2000). Driving AMPA receptors into synapses by LTP and CaMKII: requirement for GluR1 and PDZ domain interaction. Science *287*, 2262–2267.

Hosokawa, T., Saito, T., Asada, A., Fukunaga, K., and Hisanaga, S. (2010). Quantitative measurement of in vivo phosphorylation states of Cdk5 activator p35 by Phos-tag SDS-PAGE. Mol. Cell. Proteomics *9*, 1133–1143.

Kameyama, K., Lee, H.K., Bear, M.F., and Huganir, R.L. (1998). Involvement of a postsynaptic protein kinase A substrate in the expression of homosynaptic long-term depression. Neuron *21*, 1163–1175.

Kim, M.J., Futai, K., Jo, J., Hayashi, Y., Cho, K., and Sheng, M. (2007). Synaptic accumulation of PSD-95 and synaptic function regulated by phosphorylation of serine-295 of PSD-95. Neuron *56*, 488–502.

Kinoshita, E., Kinoshita-Kikuta, E., Matsubara, M., Yamada, S., Nakamura, H., Shiro, Y., Aoki, Y., Okita, K., and Koike, T. (2008). Separation of phosphoprotein isotypes having the same number of phosphate groups using phosphate-affinity SDS-PAGE. Proteomics *8*, 2994–3003.

Lee, H.K., Barbarosie, M., Kameyama, K., Bear, M.F., and Huganir, R.L. (2000). Regulation of distinct AMPA receptor phosphorylation sites during bidirectional synaptic plasticity. Nature *405*, 955–959.

Lee, H.K., Takamiya, K., Han, J.S., Man, H., Kim, C.H., Rumbaugh, G., Yu, S., Ding, L., He, C., Petralia, R.S., et al. (2003). Phosphorylation of the AMPA receptor GluR1 subunit is required for synaptic plasticity and retention of spatial memory. Cell *112*, 631–643.

Lee, H.K., Takamiya, K., Kameyama, K., He, K., Yu, S., Rossetti, L., Wilen, D., and Huganir, R.L. (2007). Identification and characterization of a novel phosphorylation site on the GluR1 subunit of AMPA receptors. Mol. Cell. Neurosci. *36*, 86–94.

Li, A.J., Suzuki, M., Suzuki, S., Ikemoto, M., and Imamura, T. (2003). Differential phosphorylation at serine sites in glutamate receptor-1 within neonatal rat hippocampus. Neurosci. Lett. *341*, 41–44.

Lu, W., Man, H., Ju, W., Trimble, W.S., MacDonald, J.F., and Wang, Y.T. (2001). Activation of synaptic NMDA receptors induces membrane insertion of new AMPA receptors and LTP in cultured hippocampal neurons. Neuron *29*, 243–254.

Lu, W., Isozaki, K., Roche, K.W., and Nicoll, R.A. (2010). Synaptic targeting of AMPA receptors is regulated by a CaMKII site in the first intracellular loop of GluA1. Proc. Natl. Acad. Sci. USA *107*, 22266–22271.

Mitsushima, D., Ishihara, K., Sano, A., Kessels, H.W., and Takahashi, T. (2011). Contextual learning requires synaptic AMPA receptor delivery in the hippocampus. Proc. Natl. Acad. Sci. USA *108*, 12503–12508.

Mitsushima, D., Sano, A., and Takahashi, T. (2013). A cholinergic trigger drives learning-induced plasticity at hippocampal synapses. Nat. Commun. *4*, 2760.

Miyazaki, T., Takase, K., Nakajima, W., Tada, H., Ohya, D., Sano, A., Goto, T., Hirase, H., Malinow, R., and Takahashi, T. (2012). Disrupted cortical function underlies behavior dysfunction due to social isolation. J. Clin. Invest. *122*, 2690–2701.

Oh, M.C., Derkach, V.A., Guire, E.S., and Soderling, T.R. (2006). Extrasynaptic membrane trafficking regulated by GluR1 serine 845 phosphorylation primes AMPA receptors for long-term potentiation. J. Biol. Chem. *281*, 752–758.

Roche, K.W., O'Brien, R.J., Mammen, A.L., Bernhardt, J., and Huganir, R.L. (1996). Characterization of multiple phosphorylation sites on the AMPA receptor GluR1 subunit. Neuron *16*, 1179–1188.

Sheng, M., and Hoogenraad, C.C. (2007). The postsynaptic architecture of excitatory synapses: a more quantitative view. Annu. Rev. Biochem. *76*, 823–847.

Shepherd, J.D., and Huganir, R.L. (2007). The cell biology of synaptic plasticity: AMPA receptor trafficking. Annu. Rev. Cell Dev. Biol. *23*, 613–643.

Steiner, P., Higley, M.J., Xu, W., Czervionke, B.L., Malenka, R.C., and Sabatini, B.L. (2008). Destabilization of the postsynaptic density by PSD-95 serine 73 phosphorylation inhibits spine growth and synaptic plasticity. Neuron *60*, 788–802.

Sumioka, A., Yan, D., and Tomita, S. (2010). TARP phosphorylation regulates synaptic AMPA receptors through lipid bilayers. Neuron *66*, 755–767.

Tanaka, J., Matsuzaki, M., Tarusawa, E., Momiyama, A., Molnar, E., Kasai, H., and Shigemoto, R. (2005). Number and density of AMPA receptors in single synapses in immature cerebellum. J. Neurosci. *25*, 799–807.

Whitlock, J.R., Heynen, A.J., Shuler, M.G., and Bear, M.F. (2006). Learning induces long-term potentiation in the hippocampus. Science *313*, 1093–1097.